Context-Dependent Nature of Destabilizing Mutations on the Stability of FKBP12†

Ewan R. G. Main, Kate F. Fulton, and Sophie E. Jackson*

Cambridge University Chemical Laboratory, Lensfield Road, Cambridge CB2 1EW, U.K.

Received December 18, 1997; Revised Manuscript Received February 20, 1998

ABSTRACT: The context-dependent nature in which mutations affect protein stability was investigated using the FK506-binding protein, FKBP12. Thirty-four mutations were made at sites throughout the protein, including residues located in the hydrophobic core, the β-sheet, and the solvent-exposed face of the α-helix. Urea-induced denaturation experiments were used to measure the change in stability of the mutants relative to that of the wild type ($\Delta\Delta G_{U-F}$). The results clearly show that the extent of destabilization, or stabilization, is highly context-dependent. Correlations were sought in order to link $\Delta\Delta G_{U-F}$ to various structural parameters. The strongest correlation found was between $\Delta\Delta G_{U-F}$ and *N*, the number of methyl-(ene) groups within a 6 Å radius of the group(s) deleted. For mutations of buried hydrophobic residues, a correlation coefficient of 0.73 ($n = 16$,where n is the number of points) was obtained. This increased to 0.81 ($n = 24$) on inclusion of mutations of partially buried hydrophobic residues. These data could be superimposed on data obtained for other proteins for which similarly detailed studies have been performed. Thus, the contribution to stability from hydrophobic side chains, independent of the extent to which a side chain is buried, can be estimated quantitatively using *N*. This correlation appears to be a general feature of all globular proteins. The effect on stability of mutating polar and charged residues in the α-helix and β-sheet was also found to be highly context-dependent. Previous experimental and statistical studies have shown that specific side chains can stabilize the N-caps of α-helices in proteins. Substitutions of Ile56 to Thr and Asp at the N-cap of the α-helix of FKBP12, however, were found to be highly destabilizing. Thus, the intrinsic propensities of an amino acid for a particular element of secondary structure can easily be outweighed by tertiary packing factors. This study highlights the importance of packing density in determining the contribution of a residue to protein stability. This is the most important factor that should be taken into consideration in protein design.

To design novel proteins, or rationally alter existing ones, a quantitative understanding of the factors that affect the stability of the native state is required. For proteins without disulfide bonds, noncovalent interactions—such as hydrophobic interactions, hydrogen bonds, and electrostatic interactions—determine protein stability (*1*). Protein engineering studies have provided an abundance of information on the relationship between protein structure and stability. Studies on hydrophobic groups (*2*−*13*) have shown that the packing of nonpolar groups and burial of hydrophobic surface area are the dominant forces in the stabilization of proteins. Studies on both fully and partially buried hydrophobic residues in barnase, CI2, and staphylococcal nuclease have shown correlations between the change in protein stability upon mutation ($\Delta\Delta G_{U-F}$) and both the packing density [number of methyl(ene) groups within a certain radius of the nonpolar groups removed] (*4*, *8*, *11*, *12*) and the difference in solvent accessible surface area that is buried on folding between wild-type and mutant side chains (*8*, *11*, *12*). Studies on T4 lysozyme (*6*) also found a correlation between $\Delta\Delta G_{U-F}$ and the size of the cavity created on truncation of the hydrophobic side chain. Other studies on β-sheets (*14*, *15*) and α-helices (*8*, *16*−*18*) have tried to establish similar correlations and, in some cases, establish the intrinsic propensities for each amino acid toward an element of secondary structure. In contrast with the hydrophobic core mutants discussed above, no correlations were observed for β-sheet mutants (*14*) and α-helix mutants (L. S. Itzhaki and A. R. Fersht, personal communication) in CI2, although a correlation between $\Delta\Delta G_{U-F}$ and the change in solvent accessible hydrophobic surface area was found for α-helix mutants in barnase (*18*). It is clear from these studies that the effects of mutations are highly context-dependent. In this paper, we investigate the context-dependent nature of a wide range of mutations in the FK506-binding protein, FKBP12.

FKBP12 is a monomer of 107 residues and, under equilibrium conditions, reversibly unfolds in a simple two-state manner (*19*). It has no disulfide bridges, and its structure has been solved by both X-ray crystallography and NMR spectroscopy (*20*, *21*). In addition, there is little evidence for significant residual structure in the denatured state (*22*). Residual structure in denatured states can lead to difficulties in the interpretation of protein engineering experiments as mutations can affect the stability of both the unfolded and native states (*23*). Using urea-induced denaturation and fluorescence spectroscopy, we have measured the changes in the free energy of unfolding for 34 mutants and wild-

† S.E.J. is a Royal Society University Research Fellow. E.R.G.M. is supported by a BBSRC studentship. K.F.F. is supported by an Elmore Scholarship (Gonville & Caius College, Cambridge, U.K.).

* To whom correspondence should be addressed.

S0006-2960(97)03111-5 CCC: $15.00 © 1998 American Chemical Society
Published on Web 04/03/1998

type FKBP12. Correlations between the difference in the change in the free energy of unfolding between the wild-type and mutant protein ($\Delta\Delta G_{U-F}$) and various structural parameters were then assessed. On the basis of previous studies (*24*, *25*), two mutations were also made at the N-cap of the α-helix to stabilize the protein. Even these mutations were found to be destabilizing.

EXPERIMENTAL PROCEDURES

Materials

Chemicals. The buffer used in the denaturation experiments was Trizma-HCl purchased from Sigma. Ultragrade urea was purchased from Fisher Scientific U.K. Ltd. Water was purified to 15 MΩ resistance by an Elgastat system. The enzymes T4 polynucleotide kinase and PFU DNA polymerase and their buffers were purchased from Stratagene. T4 DNA ligase and buffer were purchased from New England Biolabs. All other chemicals were purchased from Sigma.

Mutagenesis. Site-directed mutagenesis was carried out using inverse PCR techniques on pGST-FKBP12, a high-level *Escherichia coli* expression vector (*26*). Mutants were identified by direct sequencing of the plasmids. Plasmids containing the correct mutation were transformed into *E. coli* BL21 cells for expression.

Methods

Expression and Purification of the Wild Type and Mutants. Both wild-type and mutant FKBP12 were expressed and purified using the protocol described elsewhere (*26*). The identity and purity of the mutant proteins was confirmed by SDS−PAGE and electrospray mass spectrometry.

Spectroscopy. The intrinsic fluorescence of FKBP12 increases on denaturation and can be used to probe the state of folding of the protein. The change in the fluorescence has been shown to correspond to a global denaturation of the protein (*19*). An excitation wavelength of 280 nm and an emission wavelength of 356 nm were used. A Perkin-Elmer Luminescence LS50B spectrometer was used for the urea denaturation studies, with a band-pass of 10 nm.

Chemical Denaturation Experiments. Urea solutions were prepared gravimetrically in volumetric flasks. These solutions were flash-frozen in 30 mL aliquots and stored at −20 °C. Each aliquot, once thawed, was split and diluted into a large number of 800 μL aliquots of different urea concentrations using a Hamilton Microlab apparatus. For each data point in the denaturation curve, 100 μL of a FKBP12 stock solution [18 μM FKBP12, 450 mM Tris-HCl, and 9 mM DTT (pH 7.5)] was added to 800 μL of the appropriate denaturant. The protein/denaturant solutions were pre-equilibrated at 25 °C for approximately 1 h. Spectroscopic measurements were carried in a thermostated cuvette holder at 25 °C, and the temperature was monitored throughout the experiment. Urea-induced denaturation of FKBP12 has been shown to be completely reversible (*19*).

Data Analysis

(i) Calculation of m and $[D]_{50\%}$. It has been found experimentally that the free energy of unfolding of proteins in the presence of a chemical denaturant is linearly related to the concentration of that denaturant (*27*, *28*):

$$\Delta G_{U-F}{}^{D} = \Delta G_{U-F}{}^{H_2O} - m[D] \quad (1)$$

where $\Delta G_{U-F}{}^{D}$ is the free energy of unfolding at a particular denaturant concentration, $\Delta G_{U-F}{}^{H_2O}$ is the free energy of unfolding in water, m is a constant that is proportional to the increase in degree of exposure of the protein on denaturation, and [D] is the concentration of denaturant. From eq 1, we can derive eq 2:

$$F = \frac{(\alpha_N + \beta_N[D]) + [(\alpha_U + \beta_U[D])\exp[[m([D] - [D]_{50\%})]]]/RT}{1 + \exp[m([D] - [D]_{50\%})]/RT} \quad (2)$$

where F is the measured fluorescence, α_N and α_U are the intercepts and β_N and β_U are the slopes of the fluorescence baselines at low (N) and high (U) denaturant concentrations, respectively, $[D]_{50\%}$ is the concentration of denaturant at which the protein is 50% denatured, and m is the constant from eq 1. Data were fitted to eq 2 by nonlinear regression analysis using the general curve fit option in the *Kaleidagraph* program (Abelbeck Software, version 3.0). This gives the values for m and $[D]_{50\%}$ with calculated standard errors. For a more detailed description of the data analysis, see ref *11*.

(ii) Calculation of $\Delta\Delta G_{U-F}$. The value of $\Delta\Delta G_{U-F}{}^{[D]_{50\%}}$, the difference in free energy between wild-type and mutant proteins, is calculated using

$$\Delta\Delta G_{U-F}{}^{[D]_{50\%}} = \langle m \rangle \Delta[D]_{50\%} \quad (3)$$

where $\Delta[D]_{50\%}$ is the difference in the $[D]_{50\%}$ of the wild-type and mutant protein and $\langle m \rangle$ is the average value of m. Values of $[D]_{50\%}$ were found to be relatively insensitive to other variables such as sloping baselines and can be measured reproducibly to within 0.05 M. We have used a value of $\langle m \rangle$, obtained from measurements of 33 mutant proteins and wild type, of 1.59 ± 0.02 kcal mol^{-1} M^{-1}. The use of a mean m value allows $\Delta\Delta G_{U-F}{}^{[D]_{50\%}}$ to be calculated with minimum error. Values of $\Delta\Delta G_{U-F}{}^{H_2O}$, the difference in free energy between the wild-type and mutant proteins in water, can also be calculated using individual m values. These were found to be within experimental error of the values obtained using eq 3; however, the associated errors were significantly larger. The results presented here were calculated using eq 3.

Calculation of the Solvent Accessible Surface Area. The solvent accessible surface area of side and main chain groups of wild-type and mutant FKBP12 were calculated using the program *Xplor* (version 3.1). The percentage of solvent accessible surface area in the native state relative to that in the unfolded state was calculated using solvent accessible surface areas of model tripeptides (*29*).

Structure of FKBP12. The major secondary structural features of FKBP12 are a large, amphiphilic, five-stranded antiparallel β-sheet with a +3, +1, −3, −1 topology and a small, amphiphilic α-helix. The α-helix,[1] from Arg 57 to Val 63, packs against the hydrophobic face of the β-sheet to form the main hydrophobic core of the protein. The β-sheet comprises β-strand 1 (Val 2−Ser 8), β-strand 4 (Arg

71−Ile 76), β-strand 5 (Leu 97−Leu 106), β-strand 2 (Thr 21−Leu 30), and β-strand 3, which splits into two (Lys 35−Ser 38 and Phe 46−Met 49).

Description of Mutations. Mutations were made to (i) buried hydrophobic residues (Figure 1A,B), (ii) residues on the solvent-exposed face of the α-helix (Figure 1C), and (iii) residues in the β-sheet that only interact with other β-sheet residues (Figure 1D). The mutations introduced were mainly "non-disruptive deletions", i.e., mutations that truncated side chains thereby removing interactions without introducing any new ones.

(i) Buried Hydrophobic Residues. Fifteen residues were mutated, with the mutations fitting into one of the following three categories: (i) Ile → Val mutations which remove one methyl group, (ii) Val → Ala mutations which remove two methyl groups, and (iii) lle → Ala or Leu → Ala mutations which remove three methylene groups. At residues 76 and 91, both Ile → Val and Ile → Ala mutants were made.

(ii) α*-Helix and* β*-Sheet.* In most cases, multiple substitutions were made at a single position. Residues in the α-helix were mutated to Ala and Gly, while residues in the β-sheet were mutated to Ser, Val, and Ala (except for Ile 7 where a single mutation of Ile → Val was made). In addition, two further mutations were introduced at the N-cap of the α-helix in an attempt to stabilize the α-helix. Tables 1 and 2 summarize the mutants and the physical environment around the site of mutation in the native, wild-type structure.

RESULTS

Urea-Induced Denaturation

Wild-type and mutant FKBP12 proteins all follow a two-state unfolding transition under equilibrium conditions. Typical normalized urea-induced denaturation curves of the hydrophobic mutants, α-helix mutants, and β-sheet mutants are shown in panels A−C of Figure 2, respectively. Data from the transition curves were fitted to eq 2 to yield values for $[\text{urea}]_{50\%}$ and m. The results are summarized in Table 3. A mean m value, $\langle m \rangle$, of 1.59 ± 0.02 kcal mol^{-1} M^{-1} (standard error) was used to calculate $\Delta\Delta G_{\text{U-F}}^{[\text{D}]_{50\%}}$ using eq 3. It is clear from these data that $[\text{urea}]_{50\%}$ can be determined to within 0.03 M. Those mutants with higher errors, Ile → Ala 76 and Ile → Asp 56, are found to be highly destabilized. Although a range of m values is observed for the mutants studied, all values are within experimental error. Similar variations have been observed for other proteins (*8*, *11*). Of the 34 mutants studied, 19 are substitutions of buried hydrophobic residues, 6 are on the solvent-exposed face of the α-helix, and 9 make interactions exclusively within the β-sheet. These three groups are considered individually.

Buried Hydrophobic Residues

Effect of Cavity-Creating Mutations on the Stability of FKBP12 and Comparison with Other Proteins. The results obtained from the urea denaturation of FKBP12 mutants can be used to measure, with a high degree of accuracy, the effect on stability of cavity-creating mutations. The results allow one to estimate the energetic cost of deleting one (Ile → Val or Ala → Gly), two (Val → Ala), or three (Leu → Ala) methyl(ene) groups from within the core of a protein. Table 4 shows that the results obtained for FKBP12 are within the experimentally determined distributions found for other proteins.

Correlations between the Local Environment of the Mutated Residue and Stability. It is clear from the standard deviations in Table 4 that, although there is a correlation between the number of methyl(ene) groups deleted on mutation and $\Delta\Delta G_{\text{U-F}}^{[\text{D}]_{50\%}}$, there is extensive scatter about the mean. Furthermore, Table 2 shows that identical mutations at different positions in the protein yield different $\Delta\Delta G_{\text{U-F}}$ values. These variations must result from the specific environment surrounding the mutated residue. As in previous studies (*4*, *8*, *11*), correlations were sought between the $\Delta\Delta G_{\text{U-F}}$ values and various structural parameters that describe the environment surrounding the mutated residue.

The strongest correlation was found between $\Delta\Delta G_{\text{U-F}}$ and N, the number of methyl(ene) side chain groups within a radius of 6 Å of the group deleted on mutation. Several high-resolution structures for FKBP12 are available: the crystal structure in the presence (*21*) and absence (*30*) of the ligand rapamycin and an NMR solution structure (*20*). Values of N from the different structures were found to yield similar correlation coefficients; therefore, the highest-resolution structure (*21*) was used in the subsequent analysis. A correlation between $\Delta\Delta G_{\text{U-F}}$ and N has also been observed for barnase and CI2 (*8*, *11*). The correlation coefficient for FKBP12 is 0.73 (n = 16) compared with 0.90 (n = 20) for barnase and 0.84 (n = 10) for CI2, where n is the number of data points. Despite the poorer correlation, the results for FKBP12 can be superimposed on those obtained for CI2 and barnase (Figure 3A), suggesting that this is a general feature of the hydrophobic core of globular proteins. When the data for FKBP12, CI2, and barnase are combined, a correlation coefficient of 0.83 (n = 46) is obtained. For barnase and CI2, there is also a correlation, although somewhat weaker, between $\Delta\Delta G_{\text{U-F}}$ and Δsasa, the difference in the side chain solvent accessible surface area buried on folding between the wild type and mutant [correlation coefficients of 0.79 (n = 10) and 0.83 (n = 20) for barnase (*8*) and CI2 (*11*), respectively]. In comparison, little correlation is observed between $\Delta\Delta G_{\text{U-F}}$ and Δsasa for FKBP12 [correlation coefficient of 0.45 (n = 12)].

If one considers the data obtained for the deletion of both buried and partially buried hydrophobic groups, one obtains an even stronger correlation for FKBP12 [correlation coefficient of 0.81 (n = 24)]. This has also been found for CI2 [correlation coefficient of 0.86 (n = 47)] (*12*). Again, the data sets for FKBP12 and CI2 can be superimposed (Figure 3B) and, when combined, yield an overall correlation coefficient of 0.83 (n = 71). Two mutations, Ile → Ala 91 and Ile → Val 91, were not included in the analysis as this residue is in a flexible, disordered region in the native state (*20*).

[1] A certain ambiguity was found to exist when defining the N- and C-caps of the α-helix, due to different definitions of α-helix boundaries. For example, if one uses Φ and ψ angles, then the N-cap would be Arg 57 with Val 63 as the C-cap. However, if one uses the definition of Richardson and Richardson (*31*), the N-cap (or C-cap) is the first (or last) residue whose α-carbon lies approximately in the cylinder formed by the helix backbone and approximately along the helical spiral path, in which case the N-cap is Ile 56 and the C-cap is Val 63.

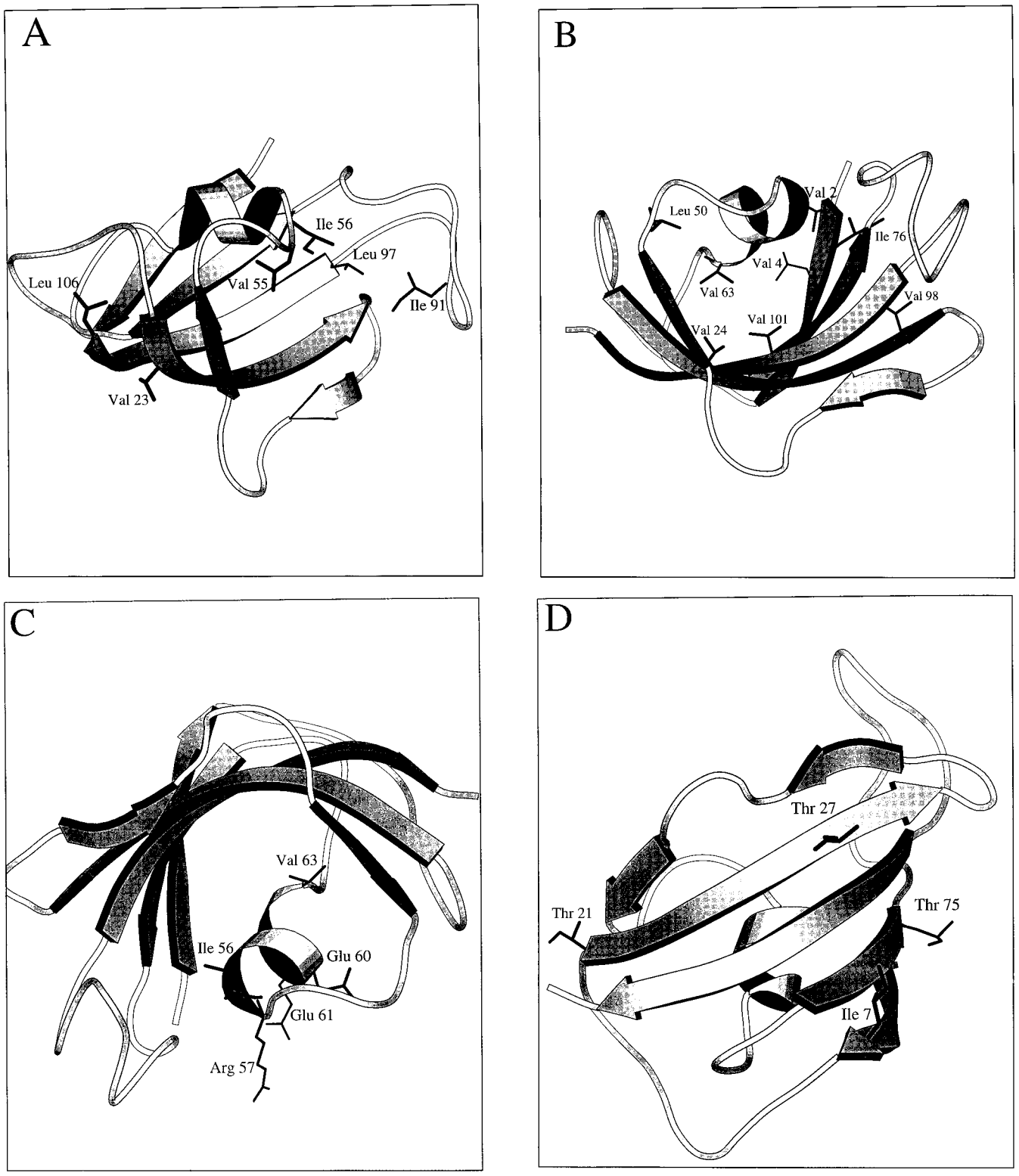

FIGURE 1: Structure of FKBP12, showing the side chains that were mutated in this study: (A and B) buried hydrophobic residues, (C) α-helix residues, and (D) *β*-sheet residues. The diagram was produced using the program *MolScript* (*37*).

α-*Helix*

Ile 56 Stabilizing Structures. Two mutations were designed in an attempt to stabilize the α-helix by either (i) introducing hydrogen bonding partners for those main chain groups at the N terminus of the helix that have unsatisfied hydrogen bonds or (ii) introducing groups which can interact favorably with the α-helix dipole. The side chain of Ile 56, which is the N-cap residue as defined by Richardson and Richardson (*31*), was mutated to Asp and Thr. However, even though these amino acids have been shown to be favored at the N-cap of α-helices (*24*, *25*), both mutants were significantly destabilized ($\Delta\Delta G_{U-F} = 3.16$ kcal mol^{-1} for Ile → Asp 56 and 1.81 kcal mol^{-1} for Ile → Thr 56). This suggests that favorable interactions that may have been

Table 1: Interactions Lost upon Mutation and the Solvent Accessible Surface Area of Buried Hydrophobic Mutants

residue	mutation	% solvent accessible surface area: main chain	% solvent accessible surface area: side chain	atoms removed on mutation	no. of methyl(ene) groups within 6 Å	side chains within 4.5 Å
Val 2	Val → Ala	63	3	Cγ1	11	Glu 61 (Cβ)
				Cγ2	13	Leu 74 (Cβ, Cγ, Cδ), Ile 76 (Cγ1)
Val 4	Val → Ala	74	4	Cγ1	11	Gln 70 (Nε2), Ala 72 (Cβ), Met 66 (Cγ), Leu 74 (Cδ1)
				Cγ2	12	Gln 65 (Cδ, Oε1, Cγ, Nε2), Leu 74 (Cγ)
Val 23	Val → Ala	0	5	Cγ1	14	Leu 104 (Cδ1), Pro 45 (Cβ), Lys 47 (Cγ, Cε)
				Cγ2	14	Lys 105 (Cβ, Cγ, Cδ), Glu 107 (Cδ, Cγ, Oε1, Oε2), Lys 47 (Cγ, Cδ, Cε)
Val 24	Val → Ala	0	0	Cγ1	17	Leu 103 (Cδ1), Val 101 (Cγ1), Cys 22 (Cβ)
				Cγ2	18	Phe 46 (Cβ), Val 101 (Cγ1), Trp 59 (Cζ3), Tyr 26 (Cδ1), Phe 46 (Cδ2)
Phe 36	Phe → Ala	75	10	Cγ	8	Ile 91 (Cδ1)
				Cδ1	8	Asp 37 (Cβ), Ile 90 (Cγ2), Ile 91 (Cδ1)
				Cδ2	9	Leu 30 (Cγ, Cδ2), Ile 91 (Cδ1)
				Cε1	12	Asp 37 (Cβ), Ile 91 (Cδ1), Phe 99 (Cε2, Cζ)
				Cε2	15	Leu 30 (Cδ2), Ile 91 (Cδ1), Leu 97 (Cδ2)
				Cζ	15	Ile 91 (Cδ1), Leu 97 (Cδ2), Phe 99 (Cε1, Cε2, Cζ)
Leu 50	Leu → Ala	0	0	Cγ	12	Glu 60 (Oε1)
				Cδ1	13	Phe 48 (Cε2, Cζ), Glu 60 (Oε1)
				Cδ2	8	Pro 16 (Cβ), Ala 64 (Cβ)
Val 55	Val → Ala	6	9	Cγ1	18	Phe 46 (Cε2, Cζ), Phe 48 (Cβ, Cγ, Cδ2), Glu 56 (Cβ)
				Cγ2	20	Phe 48 (Cγ, Cδ2, Cε2, Cζ), Trp 59 (Cβ), Glu 60 (Cγ, Cδ, Oε1)
Ile 56	Ile → Thr	16	10	Cγ1	14	Trp 59 (Cβ, Cγ, Cδ1)
	Ile → Asp			Cγ2	8	Tyr 82 (Cδ1, Cε1, Cε2, Cζ)
	Ile → Ala			Cδ1	22	Trp 59 (Cδ1), Ile 76 (Cδ1), Phe 99 (Cε1), Leu 97 (Cδ1), Ala 81 (Cβ)
Val 63.	Val → Ala	0	0	Cγ1	18	Pro 16 (Cγ), Cys 22 (Cβ, Sγ), Phe 48 (Cε1, Cζ)
				Cγ2	23	Met 66 (Sδ), Val 101 (Cγ1), Phe 48 (Cζ), Trp 59 (Cε3, Cδ2)
Ile 76	Ile → Val and Ile → Ala	0	0	Cγ1	14	Leu 74 (Cβ), Val 2 (Cβ, Cγ2), Gly 58 (Cα)
				Cγ2	12	Gly 58 (Cα), Tyr 80 (Cβ), Ala 81 (Cα, Cβ)
				Cδ1	22	Leu 74 (Cβ), Trp 59 (Cδ1, Nε1), Phe 99 (Cδ1, Cε1), Ile 56 (Cδ1), Gly 58 (Cα)
Ile 91	Ile → Val and Ile → Ala	12	1	Cγ1	20	Tyr 82 (Cε2, Cδ2), His 87 (Cβ), Ile 90 (Cβ, Cγ2; both conformations)
				Cγ2	13	Leu 97 (Cδ2), Leu 30 (Cδ2), Ala 95 (Cβ), Pro 92 (Cδ), Tyr 82 (Cβ, Cδ2)
				Cδ1	18	Phe 36 (Cγ, Cδ1, Cδ2, Cε1, Cε2, Cζ), Leu 97 (Cδ2), Leu 30 (Cδ2), Ile 90 (Cγ2)
Leu 97	Leu → Ala	0	0	Cγ	18	Phe 99 (Cε1), Ala 81 (Cβ)
				Cδ1	22	Phe 99 (Cε1, Cζ), Ile 56 (Cδ1), Tyr 82 (Cδ2, Cε2), Ala 81 (Cβ)
				Cδ2	17	Phe 36 (Cε2, Cζ), Leu 30 (Cδ2), Ile 91 (Cγ2, Cδ1), Ala 95 (Cβ)
Val 98	Val → Ala	1	8	Cγ1	11	Thr 75 (Oγ1), Met 29 (Sδ, Cγ, Cε)
				Cγ2	7	Met 29 (Sδ, Cγ, Cε), Lys 73 (Cγ, Cε, Nζ), NB (two conformations)
Val 101	Val → Ala	0	0	Cγ1	17	Val 24 (Cβ, Cγ1, Cγ2), Val 63 (Cγ2), Met 66 (Sδ), Trp 59 (Cη2)
				Cγ2	21	Tyr 26 (Cβ), Trp 59 (Cε2, Cζ2, Ch2), Phe 99 (Cβ), Leu 74 (Cδ1, Cδ2)
Leu 106	Leu → Ala	52	6	Cγ	14	Val 68 (Cγ2), Gln 20 (Nε2, Oε1)
				Cδ1	11	Thr 14 (Cγ2), Val 68 (Cγ2), Gln 20 (Nε2, Cδ, Oε1)
				Cδ2	11	Leu 103 (Cδ1), Pro 16 (Cγ, Cα, Cβ), Gln 20 (Oε1), Cys 22 (Cα, Cβ, Sγ)

introduced on mutation are more than outweighed by the loss of favorable interactions, resulting in a net destabilization of the protein.

Arg 57, Glu 60, and Glu 61. The mutations of Arg 57, Glu 60, and Glu 61 to Ala and Gly remove numerous interactions, such as salt bridges, hydrogen bonds, and many favorable van der Waals contacts. It is therefore difficult to interpret the results of these mutations directly. These data can be used, however, to obtain values for $\Delta\Delta G_{U-F}$ for a "hypothetical" mutation from Ala → Gly at each position. Values for $\Delta\Delta G_{U-F}$ are 1.47, 0.71, and 1.64 kcal mol^{-1} for positions 57, 60, and 61, respectively. It is clear that removal of a methyl group at each position in the α-helix destabilizes the protein significantly and the amount of destabilization is context-dependent. This highlights the importance to α-helix stability of burying hydrophobic surface area and

Table 2: Interactions Lost upon Mutation and the Solvent Accessible Surface Area of α-Helix and β-Sheet Mutants

residue	mutation	% solvent accessible surface area: main chain	% solvent accessible surface area: side chain	atoms removed on mutation	no. of methyl(ene) groups within 6 Å	side chains within 4.5 Å
			α-Helix			
Arg 57	Arg → Ala Arg → Gly	14	63 (Cβ = 19%)	Cβ	12	Tyr 80 (Cγ, Cδ2)
				Cγ		Glu 61 (Cδ, Oε2), Tyr 80 (Cγ, Cδ2, Cε2)
				Cδ		Tyr 80 (Cγ, Cδ1, Cδ2, Cε1, Cε2, Cζ)
				Nε		Glu 61 (Oε2), Glu 61 (Cδ, Oε1, Oε2), Tyr 80 (Cδ2, Cε1, Cε2, Cζ, Oη)
				Cζ		Tyr 80 (Cε1, Cε2, Cζ, Oη), Glu 61 (Oε2)
				Nη1		Tyr 80 (Cε1, Cζ, Oη)
				Nη2		Glu 61 (Cδ, Oε2), Tyr 80 (Cζ, Oη)
Glu 60	Glu → Ala Glu → Gly	3	14 (Cβ = 17%)	Cβ	7	Val 55 (Cγ2)
				Cγ		Val 55 (Cγ2)
				Cδ		Phe 48 (Cδ2, Cε2), Leu 50 (Cδ1, Cγ2), Val 55 (Cγ2), Met 49 (O), Gly 51 (N)
				Oε1		Gly 51 (N, O), Lys 52 (N), Gln 53 (N), Glu 54 (N)
				Oε2		Gln 53 (Cβ, Cγ)
Glu 61	Glu → Ala Glu → Gly	6	48 (Cβ = 4%)	Cβ	8	Val 2 (Cγ1)
				Cγ		Tyr 80 (Cε2), Arg 57 (Cγ, Nη2, Nε)
				Cδ		Tyr 80 (Cδ2, Cε2, Cζ, Oη 3.77)
				Oε1		Arg 57 (Nε 4.27)
				Oε2		Tyr 80 (Cε2), Arg 57 (Cγ, Cδ, Nε, Nη2, Cζ)
			β-Sheet			
Ile 7	Ile → Val	80	41	Cβ	8	Arg 71 (Cβ, Cγ, Cδ)
				Cγ1	4	Lys 73 (Cβ)
				Cγ2	10	Arg 71 (Cγ, Cδ, Nε)
				Cδ1		Arg 71 (Cγ, Nε) Asp 100 (Cγ, Oδ1) Lys 73 (Cβ)
Thr 21	Thr → Ser Thr → Val Thr → Ala	0	17 (Oγ1 = 29% and Cγ2 = 12%)	Oγ1	6	Glu 107 (O), Gln 20 (O), Met 49 (Cγ, Cε)
				Cγ2	10	Glu 107 (Cβ, Oε1), Lys 47 (Cβ, Cγ, Cδ); no hydrogen-bonding partners within <4.0 Å
Thr 27	Thr → Ser Thr → Val Thr → Ala	1	28 (Oγ1 = 23% and Cγ2 = 31%)	Oγ1	9	Tyr 26 (O), Arg 40 (Cδ), Ser 38 (Cβ, Oγ)
				Cγ2	8	Lys 35 (Cγ, Cδ, Cε); possible hydrogen bonds to Tyr 26 (O) (3.36 Å) and Ser 38 (Oγ) (3.05 Å)
Thr 75	Thr → Val Thr → Ala	5	18 (Oγ1 = 6% and Cγ2 = 25%)	Oγ1	12	Glu 5 (Oε1), Lys 73 (Cδ, Cγ, Cε, Nζ), Leu 74 (O), Val 98 (Cγ1)
				Cγ2	10	Val 98 (Cγ1), Glu 31 (Oε2), Thr 96 (Cγ2); possible hydrogen bonds to Leu 74 (O) (3.90 Å)

again illustrates the dependence of $\Delta\Delta G_{U-F}$ on the environment that surrounds the point of mutation. The Cβ methylene group of Arg 57 makes interactions within the α-helix, as well as interacting with other elements of structure such as loops and turns. Both sets of interactions will contribute to the observed $\Delta\Delta G_{U-F}$ for the Ala → Gly 57 mutation. The Cβ methylene groups of Glu 60 and Glu 61, however, interact almost exclusively with residues within the α-helix. In these cases, the contribution to $\Delta\Delta G_{U-F}$ is largely a result of changes in the stability of the α-helix and not tertiary packing interactions.

The far-UV circular dichroism spectra of all the α-helix mutants were found to be identical to those of wild-type FKBP12 (data not shown). Thus, there are no significant structural changes to the protein on mutation of residues in the α-helix to either Ala or Gly.

Serrano et al. (*18*) established that for barnase (i) Gly is more favorable than Ala at the N- and C-caps of α-helices but unfavorable within the helix and (ii) there is a strong correlation between $\Delta\Delta G_{U-F}$ and Δsasa, the change on mutation in solvent accessible hydrophobic surface area buried on folding. We also find that Ala → Gly mutations are destabilizing in the middle of the helix, yet we find no correlation between $\Delta\Delta G_{U-F}$ and Δsasa. The correlation observed for barnase results from the averaging of values of $\Delta\Delta G_{U-F}$ obtained for mutants with similar Δsasa values. No correlation is observed if the points are not averaged. The values of $\Delta\Delta G_{U-F}$ obtained for Ala → Gly mutations in the α-helix of FKBP12 correlate well with *N* (see Figure 3B), and this appears to be a more accurate method for determining $\Delta\Delta G_{U-F}$ than Δsasa within α-helices. From studies of helix−coil transitions in isolated peptides, it has been estimated that the difference in the change in conformational entropy between Ala and Gly on formation of an α-helix is approximately 1 kcal mol^{-1} (*32*, *33*). As a result, one would expect an additional contribution to $\Delta\Delta G_{U-F}$ of 1 kcal mol^{-1} for Ala → Gly substitutions. It is interesting to note that, despite this additional contribution, the values for $\Delta\Delta G_{U-F}$ still correlate well with *N*.

β-Sheet

The side chain of Ile 7 is partially buried and interacts only with other residues in the β-sheet (Table 2). Deletion of the Cδ methyl group (Ile → Val 7) causes a destabilization of 0.92 kcal mol^{-1}, which is within the range observed for other proteins (*12*). The data fit very well to the general correlation observed between $\Delta\Delta G_{U-F}$ and *N*, for buried hydrophobic residues (see Figure 3B).

Thr 21 and Thr 27 have similar environments in the native structure; the main chain is completely buried, and the side

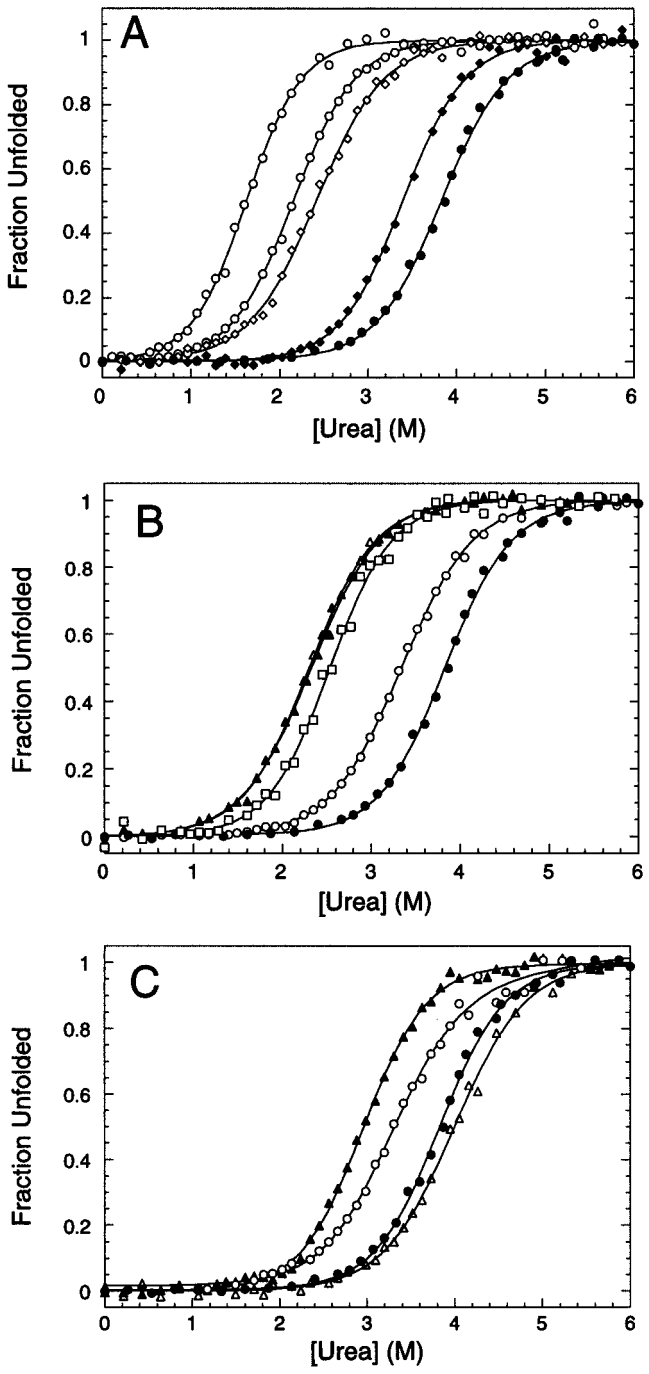

FIGURE 2: Typical urea-induced denaturation curves of wild-type (●) and mutant FKBP12 in 50 mM Tris-HCl and 1 mM DTT at pH 7.5 and 25 °C: (A) buried hydrophobic residues (IV76, ◆; LA97, ○; VA101, □; and LA106, ◇), (B) α-helix residues (EA61, ○; EG61, △; EA60, □; and EG60, ▲), and (C) *β*-sheet residues (IV7, ○; TS21, ▲; and TV27, △).

chains are partially solvent-exposed. Mutation to Ser removes a single, partially solvent-exposed methyl group, and these mutations were therefore classified as hydrophobic deletions and included in the previous analysis. $\Delta\Delta G_{U-F}$ correlates well with *N* for these mutations. In both cases, mutation to Val results in a net stabilization of the protein (0.86 and 0.23 kcal mol^{-1} for Thr 21 and 27, respectively). Thus, the unfavorable loss of the hydrogen bonds made by the Oγ group of the Thr side chain is outweighed by the gain in favorable van der Waals contacts introduced on mutation. This suggests that the hydrogen bonds that are lost on mutation are either weak, as is the case for Thr 21, or can be replaced with a solvent molecule, as may be the case for both Thr 21 and 27. Thr → Ala 21 destabilizes the protein by 1.60 kcal mol^{-1} and Thr → Ala 27 by 1.78 kcal mol^{-1}. The values are somewhat lower than might be expected, indicating that solvent molecules may access the site of mutation and replace the lost hydrogen bonding partners.

From these results, values for $\Delta\Delta G_{U-F}$ for the composite mutations Ser → Ala and Val → Ala at positions 21 and 27 can be calculated. $\Delta\Delta G_{U-F}$ = 0.16 kcal mol^{-1} for Ser → Ala 21 and 0.29 kcal mol^{-1} for Ser → Ala 27, clearly showing the small contribution that the hydroxyl group makes to protein stability. In comparison, the values of $\Delta\Delta G_{U-F}$ for Val → Ala 21 and Val → Ala 27 are 1.85 and 2.00 kcal mol^{-1}, respectively. Thus, deleting two methyl groups significantly destabilizes the protein even when they are partially exposed to solvent.

The environment around the side chain of Thr 75 is significantly different from that of Thr 21 or Thr 27; both its main chain and side chain hydroxyl group are buried,

Table 3: Changes in the Free Energies upon Mutation As Determined by Reversible Urea Denaturation Experiments

mutant	*m* value[a] (kcal mol^{-1} M^{-1})	$[urea]_{50\%}$[a] (M)	$\Delta\Delta G_{U-F}^{[urea]_{50\%}}$[b] (kcal mol^{-1})
wild type	1.43 ± 0.05	3.87 ± 0.02	N/A
	Buried Hydrophobic Residues		
Val → Ala 2	1.54 ± 0.09	2.34 ± 0.03	2.43 ± 0.12
Val → Ala 4	1.79 ± 0.12	2.12 ± 0.03	2.78 ± 0.10
Val → Ala 23	1.63 ± 0.09	2.00 ± 0.03	2.97 ± 0.10
Val → Ala 24	1.42 ± 0.08	1.86 ± 0.04	3.19 ± 0.11
Phe → Ala 36	1.78 ± 0.18	1.64 ± 0.08	3.54 ± 0.15
Leu → Ala 50	1.62 ± 0.09	2.25 ± 0.04	2.57 ± 0.11
Val → Ala 55	1.62 ± 0.13	2.53 ± 0.05	2.13 ± 0.13
Ile → Ala 56	1.70 ± 0.19	2.31 ± 0.05	2.48 ± 0.12
Ile → Asp 56	1.56 ± 0.22	1.88 ± 0.11	3.16 ± 0.20
Ile → Thr 56	1.35 ± 0.12	2.55 ± 0.06	1.81 ± 0.13
Val → Ala 63	1.69 ± 0.10	2.00 ± 0.03	2.97 ± 0.10
Ile → Val 76	1.66 ± 0.10	3.39 ± 0.03	0.76 ± 0.12
Ile → Ala 76	1.79 ± 0.25	1.47 ± 0.10	3.81 ± 0.18
Ile → Ala 91	1.52 ± 0.04	2.90 ± 0.02	1.54 ± 0.10
Ile → Val 91	1.57 ± 0.06	3.63 ± 0.02	0.38 ± 0.11
Leu → Ala 97	1.89 ± 0.13	1.63 ± 0.04	3.56 ± 0.11
Val → Ala 98	1.48 ± 0.17	2.51 ± 0.06	2.16 ± 0.13
Val → Aal 101	1.63 ± 0.04	2.14 ± 0.02	2.75 ± 0.10
Leu → Ala 106	1.53 ± 0.09	2.41 ± 0.03	2.32 ± 0.11
	α-Helix		
Arg → Ala 57	1.56 ± 0.07	3.36 ± 0.02	0.81 ± 0.11
Arg → Gly 57	1.66 ± 0.08	2.43 ± 0.02	2.29 ± 0.10
Glu → Ala 60	1.68 ± 0.10	2.53 ± 0.03	2.13 ± 0.11
Glu → Gly 60	1.50 ± 0.120	2.08 ± 0.05	2.84 ± 0.12
Glu → Ala 6l	1.47 ± 0.05	3.34 ± 0.02	0.84 ± 0.11
Glu → Gly 61	1.57 ± 0.06	2.30 ± 0.02	2.49 ± 0.10
	β-Sheet		
Ile → Val 7	1.41 ± 0.07	3.29 ± 0.02	0.92 ± 0.11
Thr → Ser 21	1.64 ± 0.07	2.96 ± 0.02	1.44 ± 0.11
Thr → Val 21	1.44 ± 0.07	4.03 ± 0.04	−0.86 ± 0.13
Thr → Ala 21	1.63 ± 0.10	2.86 ± 0.03	1.60 ± 0.11
Thr → Ser 27	1.67 ± 0.11	2.93 ± 0.03	1.49 ± 0.11
Thr → Val 27	1.61 ± 0.06	4.01 ± 0.02	−0.23 ± 0.12
Thr → Ala 27	1.55 ± 0.23	2.63 ± 0.09	1.97 ± 0.17
Thr → Val 75	1.47 ± 0.15	3.36 ± 0.05	0.81 ± 0.13
Thr → Ala 75	1.66 ± 0.12	2.20 ± 0.04	2.65 ± 0.11

[a] Calculated by fitting urea-induced denaturation data to eq 2. [b] Calculated using eq 3. All errors are calculated from the best of the data and not standard deviations from repetitive runs, unless otherwise stated.

Table 4: Average Change in Free Energy of Unfolding upon Mutation ($\Delta\Delta G_{U-F}^{[D]_{50\%}}$)

protein	Ile → Val or Ala → Gly (±SD) (kcal mol^{-1})	Val → Ala (±SD) (kcal mol^{-1})	Leu → Ala or Ile → Ala (±SD) (kcal mol^{-1})	average change in $\Delta\Delta G_{U-F}$ per methyl(ene) group (kcal mol^{-1})	reference
FKBP12[a]	1.20 ± 0.62	2.74 ± 0.35	2.72 ± 0.56	1.02 ± 0.3	N/A
barnase, staphylococcal nuclease, gene V protein	1.52 ± 0.58	2.76 ± 0.48	4.38 ± 1.39	1.45 ± 0.78	*4*, *5*, *8*
CI2	1.18 ± 0.09	3.42 ± 1.47	3.64 ± 0.60	1.33 ± 0.45	11

[a] Mutations at Ile 91 were not used (see the Discussion). Only mutants classified as nondisruptive deletions were used in this analysis.

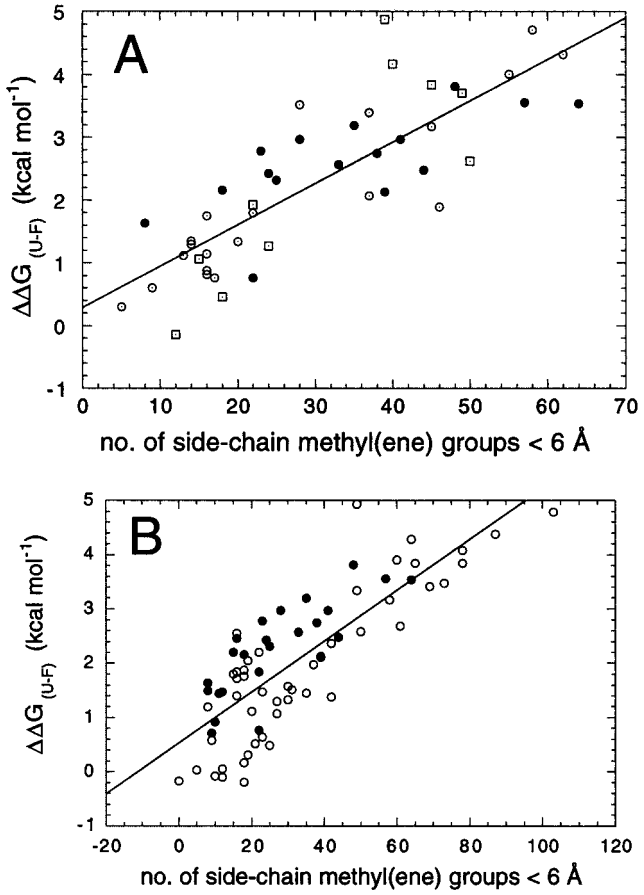

FIGURE 3: (A) Correlation between the number of side chain methyl(ene) groups within a radius of 6 Å of the group deleted and the free energy of unfolding for mutations of buried hydrophobic residues in FKBP12 (●), CI2 (□), and barnase (○). The solid line shows the best fit of the combined data to a linear equation. For FKBP12 (intercept = 1.34, slope = 0.04, R = 0.72, and number of points = 16), CI2 (intercept = −0.70, slope = 0.10, R = 0.84, and number of points = 10), barnase (intercept = 0.13, slope = 0.07, R = 0.90, and number of points = 20), and combined (intercept = 0.29, slope = 0.07, R = 0.83, and the number of points = 46). (B) Correlation between the number of side chain methyl(ene) groups within a radius of 6 Å of the group deleted and the free energy of unfolding for mutations of all hydrophobic deletions in FKBP12 (●) and CI2 (○). The solid line show the best fit of the combined data to a linear equation. For FKBP12 (intercept = 1.08, slope = 0.04, R = 0.81, and number of points = 24), CI2 (intercept = 0.16, slope = 0.05, R = 0.86, and number of points = 48), and combined (intercept = 0.53, slope = 0.05, R = 0.81, and number of points = 72).

whereas the methyl group of the side chain is partially exposed. Mutation of Thr 75 to Val and Ala results in a destabilization of 0.80 and 2.64 kcal mol^{-1}, respectively. In this case, the loss of the hydrogen bond between the Oγ of Thr 75 and the backbone of Leu 74 is significant as solvent cannot access the site of mutation. The protein is, therefore, substantially destabilized. The composite Val → Ala mutation destabilizes the protein by 1.84 kcal mol^{-1}.

For all three positions, the values of $\Delta\Delta G_{U-F}$ for the mutation of Thr → Ser and Val → Ala correlate extremely well with N (see Figure 3B).

DISCUSSION

In this study, we have analyzed 34 mutants of FKBP12 and compared the destabilization energy, $\Delta\Delta G_{U-F}$, measured by urea-induced denaturation, with various structural parameters which relate to the environment of the mutated residue in the native state. Of the 34 mutants studied, 19 are substitutions of buried hydrophobic residues, 6 are on the solvent-exposed face of the α-helix, and 9 make interactions exclusively within the β-sheet. Mutations involving deletions of buried, or partially buried, hydrophobic groups, whether these residues are in the hydrophobic core, the α-helix, or the β-sheet, can be considered together. Mutations of polar or charged side chains need to be considered separately.

All the mutations of buried hydrophobic residues were found to destabilize the protein significantly. The average destabilization energy for the deletion of one methyl(ene) group was found to be 1.0 ± 0.3 kcal mol^{-1}. This is within the range of values observed for other globular proteins (*4*, *5*, *8*, *11*). It is clear from this value, and by comparing values of $\Delta\Delta G_{U-F}$ for equivalent mutations at different positions within the protein, that the exact effect of a mutation on stability is highly context-dependent. Correlations between $\Delta\Delta G_{U-F}$ and various structural parameters were sought in a manner similar to previous studies (*4*, *8*, *11*) so we could predict with a high degree of accuracy the effect of mutation on stability.

The most significant correlation found was between $\Delta\Delta G_{U-F}$ and N, the number of methyl(ene) side chain groups within a radius of 6 Å of the group deleted on mutation. For buried hydrophobic residues, the correlation coefficient for FKBP12 is 0.73 (n = 16) and the results can be superimposed on those obtained for CI2 (*11*) and barnase (*8*) (see Figure 3A). If one considers partially buried hydrophobic side chains in addition to buried hydrophobic side chains, the correlation between $\Delta\Delta G_{U-F}$ and N is even stronger [correlation coefficient of 0.81 (n = 24), Figure 3B]. Again the data could be superimposed on similar data for CI2 (see Figure 3B). When the data for FKBP12, CI2, and barnase were combined, a correlation coefficient of 0.83 (n = 46) was obtained for completely buried hydrophobic residues and a correlation coefficient of 0.83 (n = 71) was obtained for all hydrophobic residues mutated, including partially buried residues. These results strongly suggest that the loss of stability on deletion of any hydrophobic group can be adequately explained by the packing parameter N, and

therefore the loss of van der Waals contacts. Such results strongly suggest that this correlation will hold for all globular proteins.

For mutations involving deletion of a hydrophobic group, $\Delta\Delta G_{U-F}$ can be predicted solely on the basis of *N*. For mutations involving removal of a polar or charged group, $\Delta\Delta G_{U-F}$ can be estimated from a knowledge of the solvent accessibility of the site of mutation. The energy contributed to stability by hydrogen bonds is highly variable. Buried hydrogen bonds, when lost, have the greatest destabilizing effect, as no surrogate bonding partner such as a water molecule can replace the lost interaction. Surface hydrogen bonds, on the other hand, have little or no effect on stability. Our results suggest that the loss of a buried hydrogen bond destabilizes FKBP12 by approximately 1.0−1.5 kcal mol^{-1}, which is in agreement with studies on other proteins (*34*, *35*).

It is clear from the mutations at Ile 56, the N-cap of the α-helix, that it is difficult to predict the energetic consequence of a substitution on the basis of the propensity of an amino acid for a secondary structural element alone. In this case, tertiary interactions are more important than the interactions within the element of secondary structure as has been noted elsewhere (*36*).

CONCLUSIONS

From the analysis presented here and in other studies, it is clear that the energetic cost of removing either a nonpolar, polar, or charged group from a protein is highly context-dependent. By far the most important factor contributing to protein stability is the burial of hydrophobic surface area and the concomitant formation of strong van der Waals interactions. This is true not only within the hydrophobic core of a protein, illustrating the importance of hydrophobic interactions in stabilizing tertiary structure, but also in α-helices and *β*-sheets, illustrating the importance of hydrophobic interactions in stabilizing secondary structure. We find a strong correlation between the contribution of hydrophobic groups to protein stability and their local environment by using the packing parameter *N*. This correlation is independent of both the position of the residue within the tertiary structure and the degree of burial of the residue. Such findings mirror results discovered recently for other proteins (*12*). The burial of nonpolar surface area should therefore be the prime consideration in the design of novel proteins with stable folds.

ACKNOWLEDGMENT

We thank Dr. Daniel Otzen for helpful discussions, Dr. Sarah Perrett for critically reading the manuscript, and Prof. Alan Fersht for his support.

REFERENCES

1. Dill, K. A. (1990) *Biochemistry 29*, 7133−7155.
2. Kellis, J. T. V., Nyberg, K., Sali, D., and Fersht, A. R. (1988) *Nature 333*, 784−786.
3. Kellis, J. T. V., Nyberg, K., and Fersht, A. R. (1989) *Biochemistry 28*, 4914−4922.
4. Shortle, D., Stites, W. E., and Meeker, A. K. (1990) *Biochemistry 29*, 8033−8041.
5. Sandberg, W. S., and Terwilliger, T. C. (1991) *Proc. Natl. Acad. Sci. U.S.A. 88*, 1706−1710.
6. Eriksson, A. E., Baase, W. A., Zhang, X. J., Heinz, D. W., Blaber, M., Baldwin, E. P., and Matthews, B. W. (1992) *Science 255*, 178−183.
7. Lim, W. A., Farruggio, D. C., and Sauer, R. T. (1992) *Biochemistry 31*, 4324−4333.
8. Serrano, L., Kellis, J. T., Cann, P., Matouschek, A. T. E. L., and Fersht, A. R. (1992) *J. Mol. Biol. 224*, 783−804.
9. Eriksson, A. E., Baase, W. A., and Matthews, B. W. (1993) *J. Mol. Biol. 229*, 747−769.
10. Fersht, A. R., Jackson, S. E., and Serrano, L. (1993) *Philos. Trans. R. Soc. London, Ser. A 345*, 141−151.
11. Jackson, S. E., Moracci, M., el Masry, N., Johnson, C., and Fersht, A. R. (1993) *Biochemistry 32*, 11259−11269.
12. Otzen, D. E., Rheinnecker, M., and Fersht, A. R. (1995) *Biochemistry 34*, 13051−13058.
13. Bhat, M. G., Ganley, L. M., Ledman, D. W., Goodman, M. A., and Fox, R. O. (1997) *Biochemistry 36*, 12167−12174.
14. Otzen, D. E., and Fersht, A. R. (1995) *Biochemistry 34*, 5718−5724.
15. Smith, C. K., and Regan, L. (1995) *Nature 270*, 980−982.
16. Blaber, M., Zhang, X. J., and Matthews, B. W. (1993) *Science 260*, 1637.
17. Blaber, M., Baase, W. A., Gassner, N., and Matthews, B. W. (1995) *J. Mol. Biol. 246*, 317−330.
18. Serrano, L., Neira, J. L., Sancho, J., and Fersht, A. R. (1992) *Nature 356*, 453−455.
19. Egan, D. A., Logan, T. M., Liang, H., Matayoshi, E., Fesik, S. W., and Holzman, T. F. (1993) *Biochemistry 32*, 1920−1927.
20. Michnick, S. W., Rosen, M. K., Wandless, T. J., Karplus, M., and Schreiber, S. L. (1991) *Science 252*, 836−846.
21. van Duyne, G. D., Standaert, R. F., Karplus, P. A., Schreiber, S. L., and Clardy, J. (1991) *Science 252*, 839−842.
22. Logan, T., Theriault, Y., and Fesik, S. (1994) *J. Mol. Biol. 236*, 637−648.
23. Shortle, D., and Meeker, A. K. (1989) *Biochemistry 28*, 936−944.
24. Dym, O., Mevarech, M., and Sussman, J. L. (1995) *Science 267*, 1344−1346.
25. el Masry, N., and Fersht, A. R. (1994) *Protein Eng. 7*, 777−782.
26. Jackson, S. E., Main, E. R. G., and Fulton, K. F. (1997) *J. Mol. Biol.* (submitted for publication).
27. Pace, C. N. (1986) *Methods Enzymol. 131*, 266−279.
28. Tanford, C. (1968) *Adv. Protein Chem. 23*, 121−282.
29. Miller, S., Janin, J., Lesk, A. M., and Chothia, C. (1987) *J. Mol. Biol. 196*, 641−656.
30. Wilson, K. P., Yamashita, M. M., Sintchak, M. D., Rotstein, S. H., Murcko, M. A., Boger, J., Thomson, J. A., Fitzgibbon, M. J., Black, J. R., and Navia, M. A. (1995) *Acta Crystallogr., Sect. D: Biol. Crystallogr. 51*, 511−521.
31. Richardson, J. S., and Richardson, D. S. (1988) *Science 240*, 1648−1652.
32. Stites, W. E., and Pranata, J. (1995) *Proteins: Struct., Funct., Genet. 22*, 132−140.
33. Zhang, C., Cornette, J. L., and Delisi, C. (1997) *Protein Sci. 6*, 1057−1064.
34. Chen, Y., Fersht, A., and Henrick, K. (1993) *J. Mol. Biol. 234*, 1158−1170.
35. Chen, Y. W., Henrick, K., and Fersht, A. R. (1993) *Protein Eng. 6*, 6−7.
36. Cordes, M. H. J., Davidson, A. R., and Sauer, R. T. (1996) *Curr. Opin. Struct. Biol. 6*, 3−10.
37. Kraulis, P. (1991) *J. Appl. Crystallogr. 24*, 946−950.

BI973111S